Laminar-Turbulent Transition in an Inlet Region of a Circular Pipe Induced by the Jet Disturbance

R. Nakatsu and M. Ichimiya

Department of Mechanical Engineering, Tokushima University, Tokushima 770-8506, Japan

Abstract

The laminar-turbulent transition of a boundary layer induced by a jet injection in the inlet region of a circular pipe was experimentally investigated. The jet was periodically injected radially from a small hole in the inlet region into the pipe flow. The turbulence induced by the jet within the boundary layer developed into turbulent patches which then grew in the axial, circumferential and radial directions downstream. A single hot-wire probe was used in the measurements. The axial velocity component was measured at four downstream stations, one within the inlet region and the other within the development region. Output voltage of the hot-wire was digitized and data was processed by a PC. An ensemble-averaging based on the signal from the jet trigger was performed. Mean and fluctuating velocity in the axial direction and intermittency factor which is the fraction of turbulence were obtained. In this research, three conclusions were obtained. First, the fluctuating velocity near the leading edge at the opposite side of jet hole is caused due to the crush of the jet on the wall. The fluctuation by the crush decreases downstream, though the fluctuation itself is sustained by the entrainment of the non-turbulent fluid. Second, the entrainment of the non-turbulent fluid to the turbulent patch near the trailing edge contributes to the axial growth of the patch. Third, an increase of the velocity in non-turbulent area between two patches contributes to the increase of the fluctuating velocity within and the axial growth of the turbulent patch.

Introduction

The flow within a circular pipe consists of two parts. One is an inlet region with the boundary layer and the core. The other is a development region where the boundary layer occupies the whole cross section. Fully developed laminar pipe flow, i.e., Hagen–Poiseuille flow is known to be stable to axisymmetric and all type of non-axisymmetric disturbance from theoretical and experimental results [4, 5]. However, if the Reynolds number exceeds a certain threshold level, isolated turbulent patches (turbulent puffs or slugs) originate intermittently [6]. They gradually occupy the whole cross section and their axial length grows downstream, then the flow always shows turbulence finally. The contradiction between the above fact and the linear stability theory is attributed to the ignorance of two factors in theory: finite amplitude disturbance and upstream inlet (entrance) region. Therefore, the role that the inlet region plays in the laminar-turbulent transition is significant. The present authors have conducted experiments that injected a periodic jet at upstream within the inlet region to clarify the laminar-turbulent transition mechanism. Then, the jet flow rate [1] which produces a turbulent patch, the property of the patch [2] and the relation with the surrounding laminar boundary layer [3] have been clarified. Downstream, however, near the development region, the patch had grown axially, then amalgamated with adjacent patches. This made for unclear the interaction with the surrounding laminar flow across the leading and trailing edge of the patch. Therefore, in the present investigation, the jet was injected in the downstream portion of the inlet region. Then the generated turbulent patches were investigated from the inlet to the developed region.

Experimental Apparatus and Methods

The experimental apparatus is the same one used in the previous paper [1]. A plexiglas pipe with a diameter, $D = 2a$, of 60 mm and a total length of approximately 6.2 m (= 104D) was used in the experiments. The axial velocity was axisymmetric. The coordinate system and flow field are shown in figure 1. A single jet flow was injected perpendicularly to the main flow through 2 mm diameter hole 4107 mm downstream of the coordinate origin, as shown in figure 1. Air from an air pump is led to a solenoid valve and then periodically injected in the pipe. The duration of the jet injection was kept at 0.1 second, whereas that for non-injection was 0.4 or 0.8 second. The jet flow rate was set to 1.25×10^{-5} m^3/s (jet speed $v_j \cong 4.0$ m/s), which sufficiently exceeds the threshold flow rate [1]. The ratio of flow rate between the jet and main flow is 0.003. The Reynolds number based on the pipe diameter and the velocity averaged over the cross section, U_a, is kept at 6000 ($U_a \cong 1.5$ m/s). A single hot-wire probe with a tungsten sensing element 5 μm in diameter and 1 mm in length was used in the measurements.

Axial velocity component was measured at four downstream stations, $(x-x_j)/D = 3.5$ within the inlet region and 9.4, 14.9 and 19.2 within the development region. The output voltage from the hot wire had been digitized at a 10 kHz sampling frequency and a 52 and a 104 seconds sampling period at $(x-x_j)/D = 3.5$ and three downstream stations, respectively. A 130-times ensemble-averaging based on the trigger signal was performed.

Result and Discussion

Figure 2 shows the contour maps of the fraction of the turbulent patch, intermittency factor, γ, on the diametrical planes which pass through the jet hole ($\theta = 0°$, $y = 0$), the pipe center axis and the wall of $\theta = 180°$. The numerical value in the ordinate is a height measured from the surface of the jet-hole side ($\theta = 0°$) wall normalized by the pipe radius, a. That in the abscissa is an elapsed time normalized by cross-sectional average velocity and the pipe diameter, $T = U_a(t + nT_j)/D$ (n is an integer lager than or equal to zero). The left (small T) or right (large T) sides
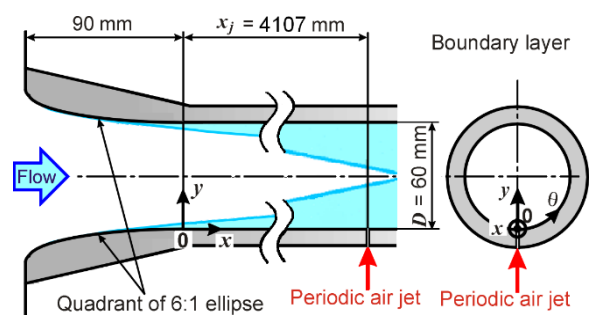
Figure 1 Coordinate system.

correspond to the leading or trailing edge sides of the turbulent patch, respectively. At $(x$-$x_j)/D = 3.5$, figure 2(a), the turbulent patch exists apart from the wall on the $\theta = 0°$ side (lower half part). Since this station is the nearest from the jet hole, the radial motion of the jet which perpendicularly injected from the hole is dominant there. Downstream at $(x$-$x_j)/D = 9.4$, 14.9, and 19.2, the patch grows both in the axial and radial directions. In addition, at $(x$-$x_j)/D = 14.9$, the shape of the patch on $\theta = 0°$ side is almost the same as that on the $\theta = 180°$ side (upper half part). At $(x$-$x_j)/D = 19.2$, the patch on $\theta = 180°$ side is longer in the upstream direction than on the $\theta = 0°$ side.

Figure 3 shows the intermittency contour maps in the cross section perpendicular to the pipe axis. These figures are shown at the center-of-gravity time with the intermittency contour maps in figure 2. The jet injection hole $\theta = 0°$ is the bottom position in each figure. The jet was injected from that position upward. Although only the half circumferential range $0° \leqq \theta \leqq 180°$ (right half of each figure) was measured, the maps are drawn for the whole circumferential range by drawing the left half symmetrically. At $(x$-$x_j)/D = 3.5$, figure 3(a), the turbulent patch crushed the wall of $\theta = 180°$ side and spreads in the circumferential direction. Farther downstream, at $(x$-$x_j)/D = 9.4$, figure 3(b), the turbulent patch keeps spreading in the circumferential direction. At $(x$-$x_j)/D = 14.9$ and 19.2, figure 3(c) and (d), the patch further spreads in the circumferential direction and the cross section is totally occupied with the patch at the center of gravity time.

Figure 4 shows the contour maps of the ensemble-averaged velocity on the diametrical planes. In figure 4(a), the turbulent patch is lifted upward in the region of $2 \leqq T \leqq 4$, due to the

radial motion of the jet. Downstream, $(x$-$x_j)/D = 14.9$ and 19.2, the patch is not lifted, due to the attenuation of the radial motion of the jet.

Figure 5 shows the contour maps of fluctuating velocity on the diametrical planes. Near the leading edge on $\theta = 180°$ side at $(x$-$x_j)/D = 3.5$, the fluctuating velocity is very large. The large fluctuation may be caused by the crush of the jet to the wall on the opposite side. On the other hand, on the $\theta = 0°$ side at $(x$-$x_j)/D = 3.5$, a moderately fluctuating region exists near the leading and trailing edges. The turbulent patch in this $\theta = 0°$ side may be induced by the jet. At $(x$-$x_j)/D = 9.4$, figure 5(b), the area of large fluctuating velocity exists near the trailing edge on the $\theta = 0°$ side. On the $\theta = 180°$ side, large and moderate fluctuations exist at the leading and trailing edges, respectively. In addition, in the non-turbulent region outside of the patch, there are slightly large fluctuating velocities near the leading and trailing edges at $\theta = 0°$ and 180°, respectively. At $(x$-$x_j)/D = 14.9$ and 19.2, figure 5(c) and (d) the large fluctuation exists near the leading and trailing edge in the patch. Especially, the fluctuation on the $\theta = 180°$ side is larger than that on the $\theta = 0°$ side.

To investigate the mechanism of the growth of the turbulent patch into the non-turbulent fluid, the relative streamlines with respect to the leading and trailing edges are shown in figure 6 and 7, respectively. The leading and trailing edges are shown in red lines. For the streamlines, the Stokes' stream functions normalized by $U_e a^2$, were calculated. They were drawn every other 0.001 except for figure 6(a) where they were drawn every other 0.005. The arrows in the figures show the relative flow direction with respect to the leading and trailing edges. Although at $(x$-$x_j)/D = 3.5$, figure 5(a), the value of the fluctuating velocity
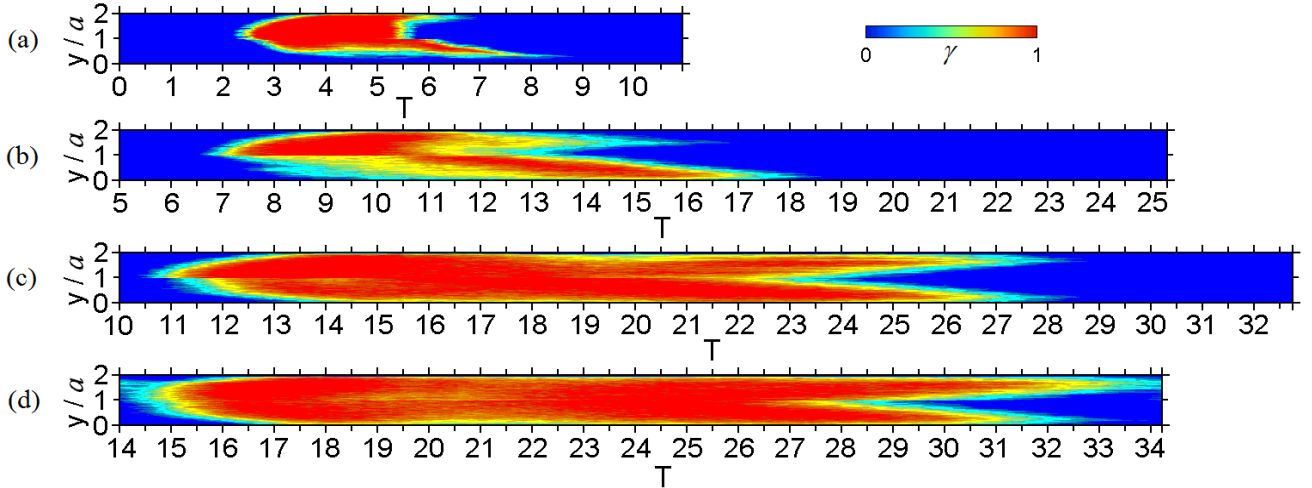
Figure 2　Intermittency contour maps on diametrical plane. (a) $(x$-$x_j)/D = 3.5$; (b) $(x$-$x_j)/D = 9.4$; (c) $(x$-$x_j)/D = 14.9$; (d) $(x$-$x_j)/D = 19.2$.
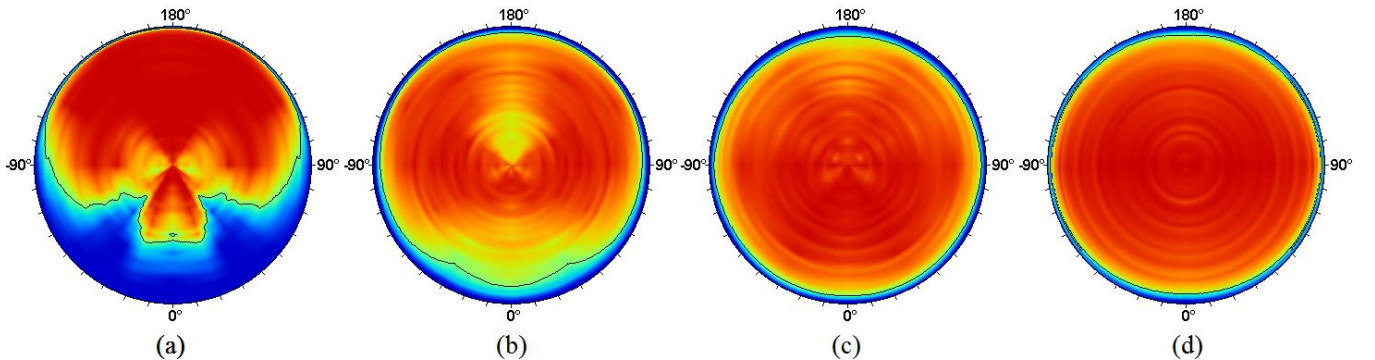
Figure 3　Intermittency contour maps on cross sections perpendicular to the pipe axis at the center of gravity time. (a) $(x$-$x_j)/D = 3.5$, $T = 4.59$; (b) $(x$-$x_j)/D = 9.4$, $T = 11.50$; (c) $(x$-$x_j)/D = 14.9$, $T = 18.66$; (d) $(x$-$x_j)/D = 19.2$, $T = 23.27$.

increased suddenly near the leading edge on the $\theta = 180°$ side, the streamline in the non-turbulent region does not enter into the leading edge on the $\theta = 180°$ side, figure 6(a). Therefore, characteristic near the leading edge on the $\theta = 180°$ side at (x-x_j)/D = 3.5 does not correspond to that of the turbulent patch at the upstream portions of the inlet region [3]. As the fluctuating region on the $\theta = 180°$ side is caused by the crush of the jet to the wall, the patch there does not indicate the characteristic of upstream portions of the inlet region [3]. Contrary to (x-x_j)/D = 3.5, the streamlines are flowing into the patch at (x-x_j)/D = 9.4 and 14.9, figure 6(b) and (c). Moreover, the large fluctuating velocity there corresponds to the characteristic of the patch of upstream portions in the inlet region [3]. Therefore, the patch which was initially affected from the crush of the jet to the wall gradually entrains non-turbulent fluid in the course of axial propagation.

In figure 7, the non-turbulent fluid near the trailing edge on the $\theta = 180°$ side is entrained from outside into the patch and the value of entrainment increased downstream. On the other hand, the entrainment near the leading edge at (x-x_j)/D = 9.4 and 14.9 decreased downstream (figure 6(b) and (c)). Therefore, the non-turbulent fluid entrained from outside at the trailing edge contributes to the axial growth of the patch. Downstream, at (x-x_j)/D =19.2, the patch entrains non-turbulent fluid with large fluctuation outside of the patch unlike the upstream portion where the small fluctuating fluid is entrained. The large fluctuation is caused by the decrease of the interval between two patches.

Conclusions

(1) The fluctuating velocity near the leading edge at the opposite side of jet hole is caused due to the crush of the jet on the wall. The fluctuation by the crush decreases downstream, though the fluctuation itself is sustained by the entrainment of the non-turbulent fluid.

(2) The entrainment of the non-turbulent fluid to the turbulent patch near the trailing edge contributes to the axial growth of the patch.

(3) An increase of the velocity in non-turbulent area between two patches contributes to the increase of the fluctuating velocity within and the axial growth of the turbulent patch.

In this research, we clarified the property of the turbulent patch. Thus we found the possibility to control the laminar-turbulent transition in the inlet region.

References

[1] Ichimiya M., Fujimura, H. & Tamatani, J., Laminar-Turbulent Transition of an Inlet Boundary Layer in a Circular Pipe Induced by Periodic Ejection (Condition for Generating an Isolated Turbulent Patch), J. Fluid Sci. Tech., 77-774, 2011, 214-226.

[2] Ichimiya M., Matsudaira, H., Fujimura, H., & Ohno, H., Laminar-Turbulent Transition of an Inlet Boundary Layer in a Circular Pipe Induced by Periodic Injection (Shape of Isolated Turbulent Patches and Their Growth), J. Fluid Sci. Tech., 79-797, 2013, 22-37.
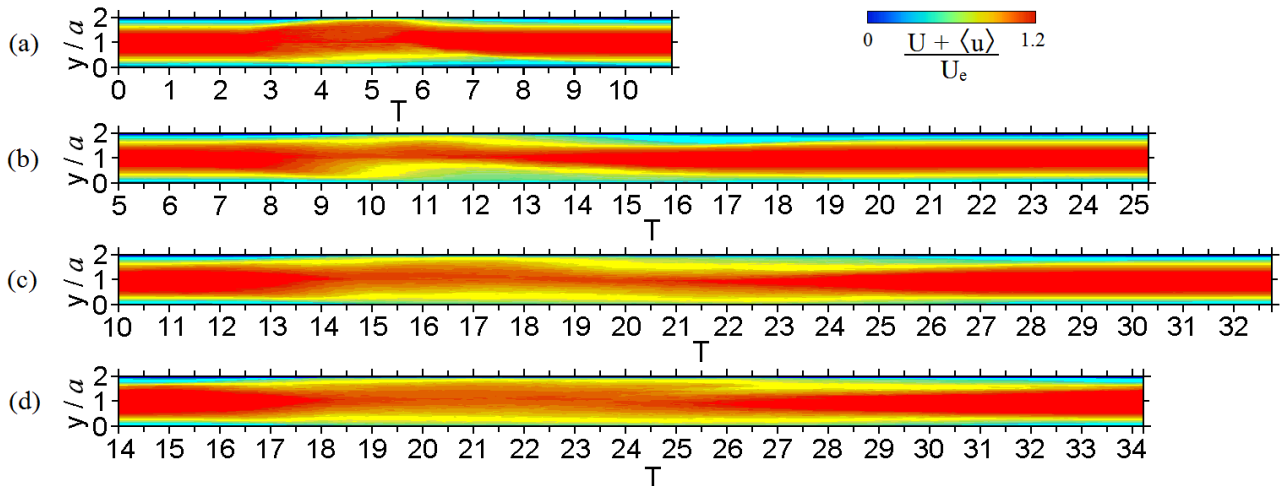
Figure 4   Contour maps of average velocity on diametrical plane. (a) (x-x_j)/D = 3.5; (b) (x-x_j)/D = 9.4; (c) (x-x_j)/D = 14.9; (d) (x-x_j)/D = 19.2.
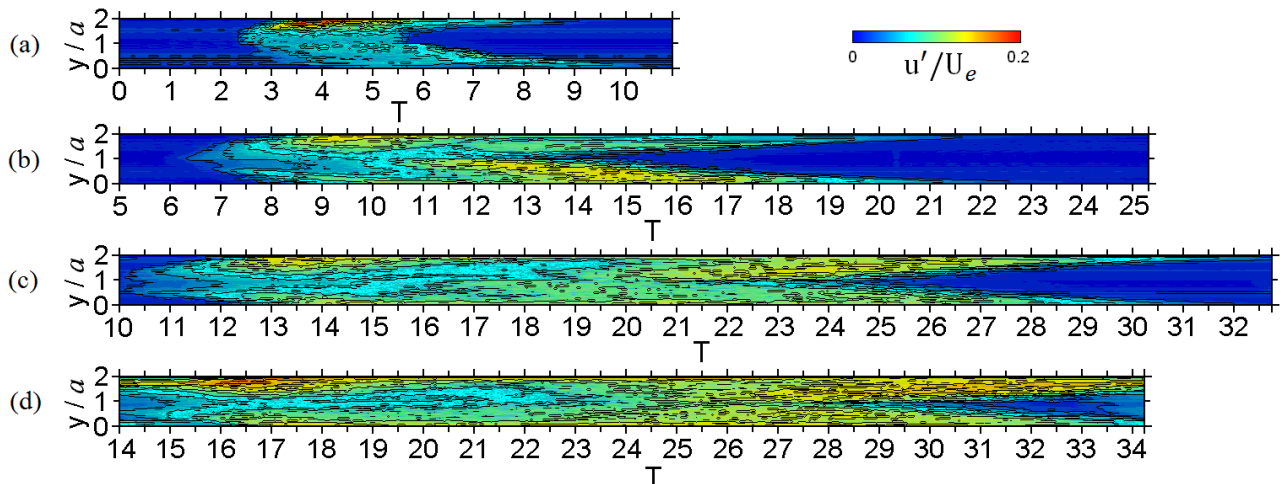
Figure 5   Contour maps of fluctuating velocity on diametrical plane. (a) (x-x_j)/D = 3.5; (b) (x-x_j)/D = 9.4; (c) (x-x_j)/D = 14.9; (d) (x-x_j)/D = 19.2.

[3] Ichimiya M., Matsudaira, H., & Fujimura, H., Laminar-turbulent transition of an inlet boundary layer in a circular pipe induced by periodic injection (Turbulence within isolated turbulent patches and its growth mechanism), J. Fluid Sci. Tech., 79-801, 2013, 863-878.

[4] Leite, R.J., An experimental investigation of the stability of Poiseuille flow, J. Fluid Mech., 5, 1959, 81-96.

[5] Sarpkaya, T., A note on the stability of developing laminar pipe flow subjected to axisymmetric and non-axisymmetric disturbances, J. Fluid Mech., 68-2, 1975, 345-351.

[6] Wygnanski. I.J. & Champagne F.H., On transition in a pipe. Part 1. The origin of puffs and slugs and the flow in a turbulent slug, J. Fluid Mech., 59-2, 1973, 281-335.

(a) $(x-x_j)/D = 3.5$

(b) $(x-x_j)/D = 9.4$

(c) $(x-x_j)/D = 14.9$
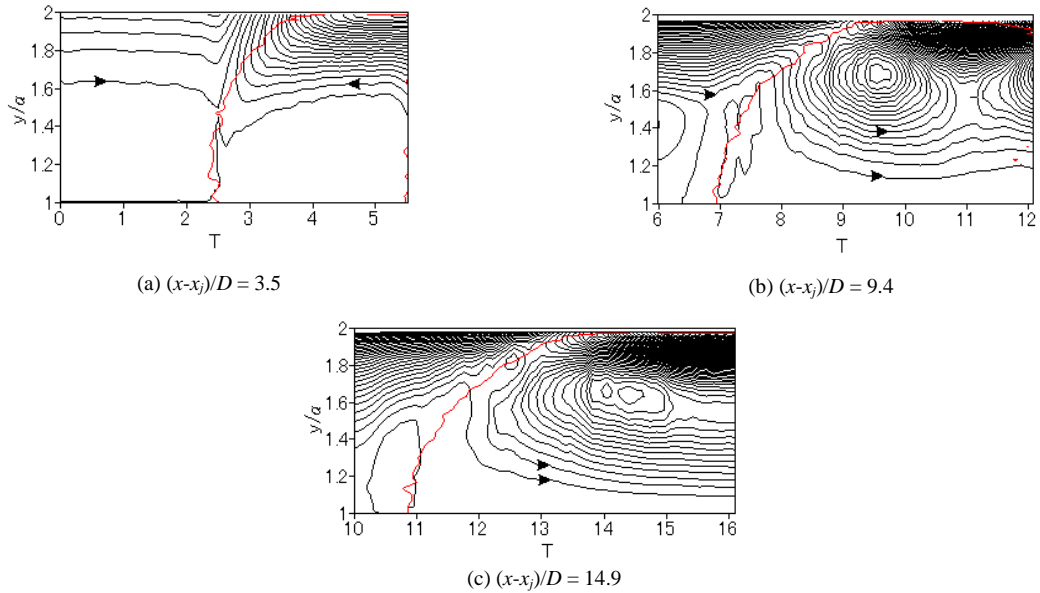
Figure 6 Streamline pattern relative to the leading interface on $\theta = 180°$ side.

(a) $(x-x_j)/D = 9.4$

(b) $(x-x_j)/D = 14.9$

(c) $(x-x_j)/D = 19.2$
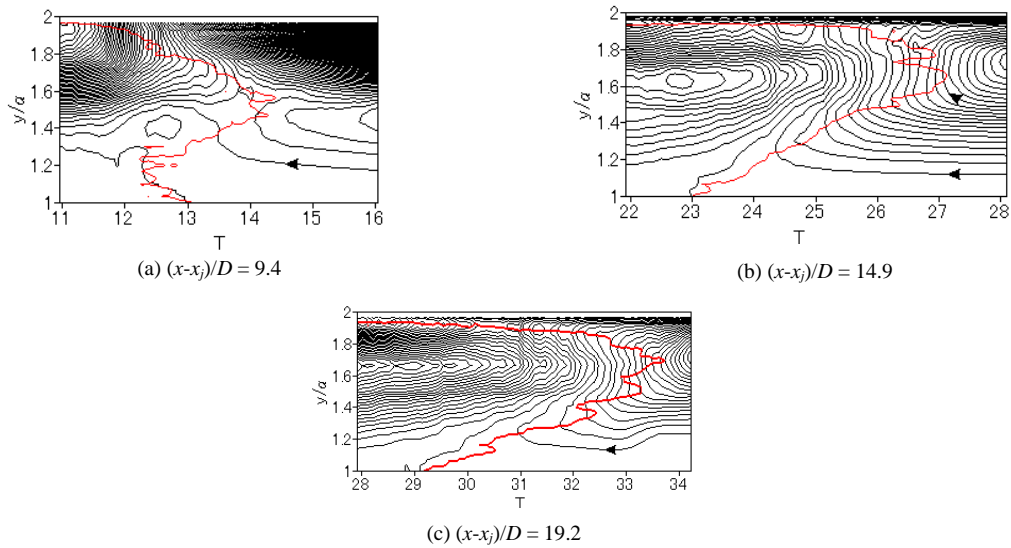
Figure 7 Streamline pattern relative to the trailing interface on $\theta = 180°$ side.